



HHS Public Access

Author manuscript

Science. Author manuscript; available in PMC 2017 January 20.

Published in final edited form as:

Science. 2014 August 29; 345(6200): 1062–1065. doi:10.1126/science.1256965.

Generation of Compartmentalized Pressure by a Nuclear Piston Governs Cell Motility in 3D Matrix*

Ryan J. Petrie^{1,*}, Hyun Koo^{1,2,3}, and Kenneth M. Yamada^{1,#}

¹Laboratory of Cell and Developmental Biology, National Institute of Dental and Craniofacial Research, National Institutes of Health, Bethesda, MD 20892-4370, USA

²Center for Oral Biology, Department of Microbiology and Immunology, University of Rochester Medical Center, Rochester, NY 14642, USA

³Biofilm Research Labs, Levy Center for Oral Health, Department of Orthodontics, University of Pennsylvania School of Dental Medicine, Philadelphia, PA

Abstract

Cells use actomyosin contractility to move through three-dimensional (3D) extracellular matrix. Contractility affects the type of protrusions cells use to migrate in 3D, but the mechanisms are unclear. Here we found that contractility generated high-pressure lobopodial protrusions in cells migrating in a 3D matrix. In these cells, the nucleus physically divided the cytoplasm into forward and rear compartments. Actomyosin contractility with the nucleoskeleton-intermediate filament linker protein nesprin 3 pulled the nucleus forward and pressurized the front of the cell. Reducing expression of nesprin 3 reduced and equalized the intracellular pressure. Thus, the nucleus can act as a piston that physically compartmentalizes the cytoplasm and increases the hydrostatic pressure between the nucleus and the leading edge to drive lamellipodia-independent 3D cell migration.

Cells moving across a flat 2D surface or inside non-linearly elastic 3D collagen use polarized signaling to direct the formation of a dendritic actin network and extend flat, lamellipodial protrusions (1, 2). When primary human fibroblasts move within a cross-linked, linearly elastic 3D structure such as dermal or cell-derived matrix, they can switch to a lamellipodia-independent migration mechanism characterized by non-polarized signaling and blunt, cylindrical protrusions termed lobopodia (1). Actomyosin contractility via the RhoA-ROCK-myosin II signaling axis is required for cells to form and maintain lobopodia in response to the degree of matrix cross-linking. However, the mechanism by which increased contractility generates lobopodia is unclear.

*This manuscript has been accepted for publication in *Science*. This version has not undergone final editing. Please refer to the complete version of record at <http://www.sciencemag.org/>. The manuscript may not be reproduced or used in any manner that does not fall within the fair use provisions of the Copyright Act without the prior, written permission of AAAS.

#Correspondence to: petrier@mail.nih.gov (R.J.P.); kyamada@mail.nih.gov (K.M.Y.).

Supplementary Materials:

Materials and Methods

Figures S1–S11

Refs 17–23

Movies S1 and S2

Lobopodial cells can also be distinguished by rapid membrane blebbing along their sides, oriented perpendicular to the leading edge. Membrane blebs can be generated by elevated intracellular hydrostatic pressure, local weakening of the attachment of the plasma membrane to the underlying cortex, or both (3–5). We hypothesized that this lateral blebbing could result from elevated intracellular pressure during lobopodial motility. This increased pressure might result from the RhoA, ROCK, and myosin II activities required for the lamellipodia-independent migration of fibroblasts through physiological linearly elastic 3D matrix (1).

We tested the hypothesis by directly determining intracellular pressures in primary human fibroblasts migrating on 2D surfaces compared to 3D extracellular matrix (ECM). We used a microelectrode coupled to a servo-null micropressure system to penetrate the plasma membrane immediately in front of the nucleus (relative to the leading edge) and to measure the intracellular hydrostatic pressure exerted by the cytoplasm directly (P_{ic} ; Fig. 1). Direct comparisons of pressure in cells migrating on top of and embedded within a 3D collagen matrix revealed low hydrostatic pressures in both 2D and 3D lamellipodial cells (~300 and 700 Pa on the linearly elastic 2D surface of cell-derived matrix (CDM) and within non-linearly elastic 3D collagen, respectively; see (1) for characterization of matrix elastic behavior). In contrast, intracellular pressure was substantially elevated (~2200 Pa) in lobopodial cells migrating inside the 3D CDM. Switching these lobopodial cells to lamellipodial by inhibiting RhoA, ROCK, or myosin II (1) reduced hydrostatic pressure (to ~400 Pa) in each case; this inhibition distinguished lobopodia from the contractility-independent water permeation mechanism used by certain cancer cells in confined channels (6). Control cells using lamellipodia to migrate on 2D glass maintained relatively low intracellular pressure (fig. S1A) with values consistent with indirect pressure estimates for other cell types (7, 8). As expected (9), placing cells in a hypotonic medium to trigger an influx of water increased P_{ic} , as did increasing contractility by treating cells with calyculin A. Thus, linearly elastic, cross-linked 3D ECM activates actomyosin contractility to increase intracellular pressure and maintain the lobopodial mode of 3D cell migration.

To establish whether intracellular pressure is uniformly increased throughout the cytoplasm of lobopodia-bearing cells, we compared hydrostatic pressures immediately in front of and behind the nucleus (Fig. 2, A and B). P_{ic} was significantly elevated and compartmentalized in lobopodia (to ~2400 Pa), with the nucleus separating this anterior high-pressure compartment from a low-pressure zone (~900 Pa) in the cell posterior. In contrast, low pressures were found both forward and back of the nucleus in fibroblasts using lamellipodia to migrate in 2D and 3D environments (~400 and 800 Pa, respectively).

The existence of large differences in hydrostatic pressure in front of versus behind the nucleus suggests that the nucleus physically divides the cytoplasm in lobopodial cells. This prediction was tested by measuring the diffusion/convection of cytoplasmic photoactivatable green fluorescent protein (PA-GFP) in live cells (Fig. 2, C and D). After photoactivation near the leading edge (Fig. 2C), fluorescent PA-GFP significantly slowed as it moved past the nucleus in lobopodial cells in 3D CDM compared to lamellipodial cells on 2D glass (Fig. 2D and fig. S2). This matrix-dependent barrier consisted of the nucleus and a dense accumulation of sheets of membranous material including endoplasmic reticulum (fig. S3).

Given the established links between the nucleus, cytoskeleton, and the ECM (10–13) and the requirement for actomyosin contractility to generate high-pressure lobopodia (Fig. 1), we hypothesized that the tight-fitting nucleus might be pulled forward like a piston to pressurize the anterior cytoplasmic compartment. Live-cell confocal microscopy showed apparent pulling forward of the nucleus, which periodically accelerated away from the cell's trailing edge in 3D CDM (movie S1). Further, monitoring of nuclear movement (NM) and P_{ic} after inhibition of myosin II revealed that the nucleus fell back and pressure equilibrated initially, ultimately becoming low and uniform (Fig. 2, E and F and movie S2), consistent with loss of actomyosin contraction pulling the nuclear piston forward. In direct contrast, the nucleus continued to move forward with no pressure change in 2D lamellipodial cells following myosin II inhibition. Microtubules were not required for nuclear movement in lobopodial cells (fig. S4).

Myosin IIA and vimentin intermediate filaments were polarized anteriorly in lobopodial cells (Fig. 3, A and B). Because nesprin 3, a nucleoskeleton-vimentin linker protein, is a proposed mediator of force transmission through the cytoskeleton to the nucleus needed for polarity and migration (14), we searched for an actomyosin-vimentin-nesprin 3 complex. Immunoprecipitation revealed an actin, myosin IIA, vimentin, and nesprin 3 complex in primary cells (Fig. 3C). Actin and myosin II were lost from the complex after inhibiting myosin II (only 18.4 \pm 12.8% (SEM) of actin and 26.7 \pm 16.3% of myosin IIA remained associated with vimentin after blebbistatin treatment, versus 88.7 \pm 14.9%, of the nesprin 3). Local inhibition of myosin II in front of the nucleus (fig. S1B) blocked forward movement of the nucleus (Fig. 2G), reduced forward pressure, and retracted the leading edge (Fig. 3D), whereas myosin II inhibition behind the nucleus did not. Similarly, local permeabilization of the plasma membrane in front of the nucleus resulted in loss of forward pressure and leading edge retraction (fig. S1C). To test whether nesprin 3 provides a link between myosin contractility and forward movement of the nucleus in lobopodial fibroblasts, we compared instantaneous velocities of the nucleus and the trailing edge in control and nesprin 3 siRNA-treated cells moving through 3D CDM (Fig. 3, E–G and fig. S5). The nucleus and trailing edge moved independently in control cells, but not in cells with reduced nesprin 3 expression (Pearson's correlation coefficient 0.28 \pm 0.01 (SEM) in control versus 0.57 \pm 0.07 in nesprin 3 siRNA-treated cells; fig. 3G and fig. S6). This loss of independent movement of the nucleus after depleting nesprin 3 was accompanied by a reduction in cell velocity similar to inhibiting global myosin II (Fig. 3H), suggesting that nesprin 3 and the nucleus are connected to a contractile pulling mechanism localized in front of the nucleus required for efficient 3D cell migration.

We tested the hypothesized role of nesprin 3 in piston function of the nucleus by depleting nesprin in cells migrating in 3D CDM. Compartmentalized forward pressure was maintained in cells treated with control siRNA, whereas siRNA knock-down of nesprin 3 reduced and equalized anterior and posterior intracellular pressures (Fig. 4A; verified with independent siRNAs in fig. S5 D and E), even though the diffusion barrier remained intact (fig. S3A). Overall actomyosin contractile function remained unaffected in nesprin 3 knock-down cells, because RhoA activation by lysophosphatidic acid (LPA) still increased 2D focal adhesion size in nesprin 3 siRNA-treated cells on glass (Fig. 4B and fig. S8). Removing the nucleus also reduced and equalized intracellular pressure, as well as slowing 3D cell movement (fig.

S7). Conversely, even though the RhoA effector formin mDia1 was required to increase focal adhesion size on 2D, its depletion did not affect the compartmentalized pressure or velocity of lobopodial cells (Fig. 3H, 4, A and B, fig. S8). Thus, nesprin 3 is required for piston-like nuclear movements and pressurizing lobopodial protrusions. This mechanism is distinct from roles of RhoA and contractility controlling focal adhesion size through mDia1.

Finally, we tested whether loss of nesprin 3 causes loss of anterior lobopodial protrusions. While control cells continued to use lobopodia to migrate through 3D CDM, the leading edges of nesprin 3 siRNA-treated cells switched to cortactin-positive lamellipodia (Fig. 4, C and D, fig. S9; confirmed with independent siRNAs in fig. S5F). This change mimics the switch from lobopodia to lamellipodia that occurs when RhoA, ROCK, or myosin II are inhibited (1), which reduced total intracellular hydrostatic pressure (Fig. 1).

Here we have shown that when human fibroblasts migrate through a physiological 3D ECM their intracellular pressure becomes compartmentalized. Furthermore, actomyosin contractility and nesprin 3 act to pull the nuclear piston forward and pressurize the anterior cytoplasmic compartment. The contractility-dependent association of vimentin intermediate filaments with nesprin 3 and actomyosin, along with the known interactions of vimentin filaments, nesprin 3, and the nucleus (14–16), supports a model in which actomyosin contractility acts on vimentin filaments to pull the nucleus forward and increase compartmentalized pressure (fig. S10). This polarized intracellular pressure is associated with a non-polarized distribution of intracellular signaling during 3D migration (1), and explains how a nucleoskeleton-cytoskeleton linker protein localized in the nuclear membrane can help to determine the structure and dynamic function of the leading edge of cells migrating in 3D ECM. This mechanism can operate in a variety of primary human cells (fig. S11) and illustrates how physical structure of the matrix can influence cellular physical properties to govern biological function.

Supplementary Material

Refer to Web version on PubMed Central for supplementary material.

Acknowledgments

We thank K. Carver for helping to characterize various primary human cells, D. Starr for providing the nesprin 3 antibody, and M. Hoffman, A. Doyle, W. Daley, and K. Holmberg for critical comments on the manuscript. This work was supported by the Intramural Research Program of the National Institute of Dental and Craniofacial Research, National Institutes of Health. The data presented in this manuscript are found in the main paper and supplementary materials and methods.

References and Notes

1. Petrie RJ, Gavara N, Chadwick RS, Yamada KM. Nonpolarized signaling reveals two distinct modes of 3D cell migration. *J. Cell Biol.* 2012; 197:439. [PubMed: 22547408]
2. Ridley AJ, et al. Cell migration: integrating signals from front to back. *Science.* 2003; 302:1704. [PubMed: 14657486]
3. Charras GT, Yarrow JC, Horton MA, Mahadevan L, Mitchison TJ. Non-equilibration of hydrostatic pressure in blebbing cells. *Nature.* 2005; 435:365. [PubMed: 15902261]
4. Tinevez JY, et al. Role of cortical tension in bleb growth. *Proc. Natl. Acad. Sci. U. S. A.* 2009; 106:18581. [PubMed: 19846787]

5. Tozluoglu M, et al. Matrix geometry determines optimal cancer cell migration strategy and modulates response to interventions. *Nat. Cell Biol.* 2013; 15:751. [PubMed: 23792690]
6. Stroka KM, et al. Water permeation drives tumor cell migration in confined microenvironments. *Cell.* 2014; 157:611. [PubMed: 24726433]
7. Charras GT, Coughlin M, Mitchison TJ, Mahadevan L. Life and times of a cellular bleb. *Biophys. J.* 2008; 94:1836. [PubMed: 17921219]
8. Dai J, Sheetz MP. Membrane tether formation from blebbing cells. *Biophys. J.* 1999; 77:3363. [PubMed: 10585959]
9. Kelly SM, Macklem PT. Direct measurement of intracellular pressure. *Am. J. Physiol.* 1991; 260:C652. [PubMed: 2003586]
10. Chambliss AB, et al. The LINC-anchored actin cap connects the extracellular milieu to the nucleus for ultrafast mechanotransduction. *Sci. Rep.* 2013; 3:1087. [PubMed: 23336069]
11. Swift J, et al. Nuclear lamin-A scales with tissue stiffness and enhances matrix-directed differentiation. *Science.* 2013; 341:1240104. [PubMed: 23990565]
12. Wolf K, et al. Physical limits of cell migration: control by ECM space and nuclear deformation and tuning by proteolysis and traction force. *J. Cell Biol.* 2013; 201:1069. [PubMed: 23798731]
13. Wu J, et al. Actomyosin pulls to advance the nucleus in a migrating tissue cell. *Biophys. J.* 2014; 106:7. [PubMed: 24411232]
14. Lombardi ML, et al. The interaction between nesprins and sun proteins at the nuclear envelope is critical for force transmission between the nucleus and cytoskeleton. *J. Biol. Chem.* 2011; 286:26743. [PubMed: 21652697]
15. Morgan JT, et al. Nesprin-3 regulates endothelial cell morphology, perinuclear cytoskeletal architecture, and flow-induced polarization. *Mol. Biol. Cell.* 2011; 22:4324. [PubMed: 21937718]
16. Wilhelmssen K, et al. Nesprin-3, a novel outer nuclear membrane protein, associates with the cytoskeletal linker protein plectin. *J. Cell Biol.* 2005; 171:799. [PubMed: 16330710]
17. Spurny R, Gregor M, Castanon MJ, Wiche G. Plectin deficiency affects precursor formation and dynamics of vimentin networks. *Exp. Cell Res.* 2008; 314:3570. [PubMed: 18848541]
18. Petrie RJ, Koo H. Direct measurement of intracellular pressure. *Curr. Protoc. Cell Biol.* 2014; 63:12.9.1. [PubMed: 24894836]
19. Dubois JM, Ouanounou G, Rouzaire-Dubois B. The Boltzmann equation in molecular biology. *Prog. Biophys. Mol. Biol.* 2009; 99:87. [PubMed: 19616022]
20. Elson EL, Qian H. Interpretation of fluorescence correlation spectroscopy and photobleaching recovery in terms of molecular interactions. *Methods Cell Biol.* 1989; 30:307. [PubMed: 2648114]
21. Michaelson D, et al. Rac1 accumulates in the nucleus during the G2 phase of the cell cycle and promotes cell division. *J. Cell Biol.* 2008; 181:485. [PubMed: 18443222]
22. Smith MB, et al. Segmentation and tracking of cytoskeletal filaments using open active contours. *Cytoskeleton.* 2010; 67:693. [PubMed: 20814909]
23. Jimenez AJ, et al. ESCRT machinery is required for plasma membrane repair. *Science.* 2014; 343:1247136. [PubMed: 24482116]

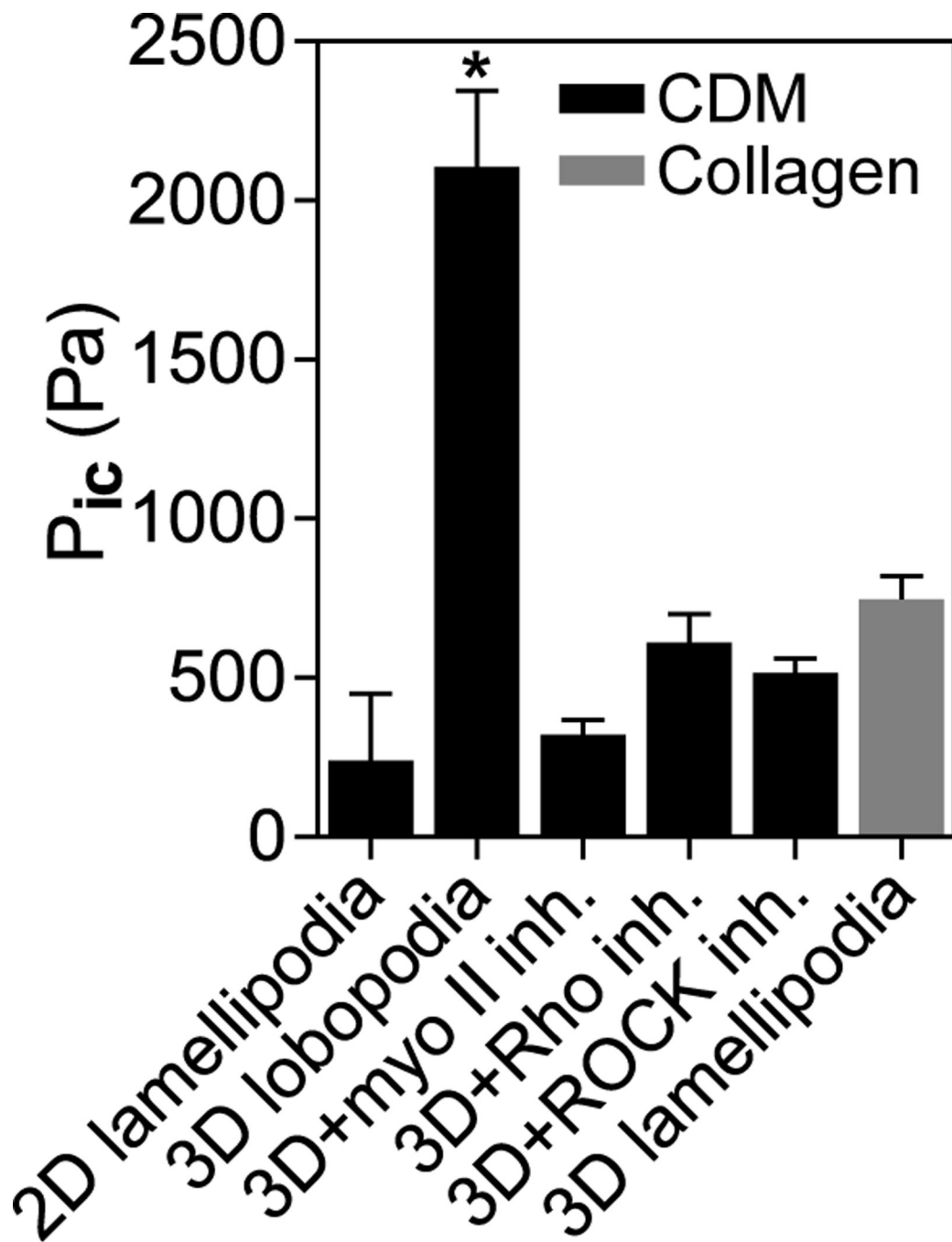


Fig. 1.

Actomyosin contractility governs intracellular pressure in 3D ECM. Comparison of the intracellular pressures ($n = 20$ each) of lamellipodial cells on 2D CDM and in 3D collagen, untreated lobopodial cells in 3D CDM, or cells in CDM treated overnight with inhibitors of myosin II (25 μ M blebbistatin, ROCK (10 μ M Y-27632), or RhoA (10 μ g/ml C3 transferase). $N=3$, $*P < 0.001$.

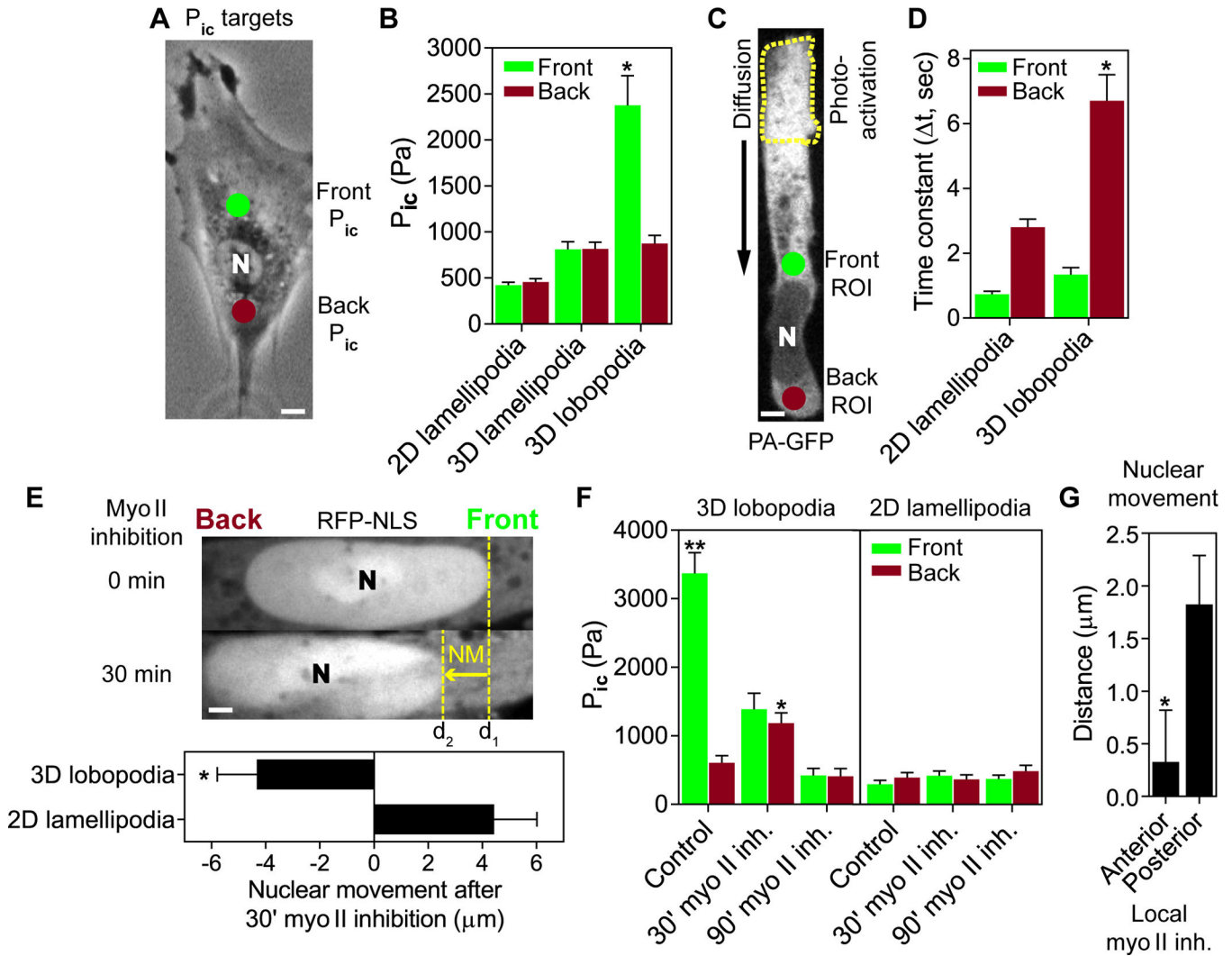


Fig. 2. Lobopodial fibroblasts are compartmentalized into high- and low-pressure zones. (A) Intracellular pressures were measured immediately in front of (green dot) and behind (red dot) the nucleus. Scale bar 5 μm . (B) Comparison of intracellular pressures in front and behind the nucleus of fibroblasts ($n = 25$) migrating on 2D glass (2D lamellipodia), in 3D collagen (3D lamellipodia), or in 3D CDM (3D lobopodia). $N=3$. (C) A sub-population of PA-GFP was activated near the leading edge (dashed line) and rate of translocation was measured at the indicated regions of interest (ROI) immediately in front of and behind the nucleus in live cells. Scale bar 5 μm . (D) Time constants of PA-GFP accumulation show that the nucleus significantly slows the rate of PA-GFP translocation in 3D lobopodial versus 2D lamellipodial fibroblasts ($n = 17$, $N=3$). (E) Myosin II inhibition results in immediate backward movement of the nucleus in lobopodial but not lamellipodial cells (quantified in the lower panel). $n=10$, $N=3$. Scale bar 3 μm . (F) Pressure rises transiently behind the nucleus following myosin II inhibition only in lobopodial cells ($n = 16$, $N=3$). $**P < 0.001$ vs. front P_{ic} , $*P < 0.01$ vs. back P_{ic} . (G) Anterior inhibition of myosin II prevents forward movement of the nucleus ($n=10$, $N=3$). $*P < 0.01$.

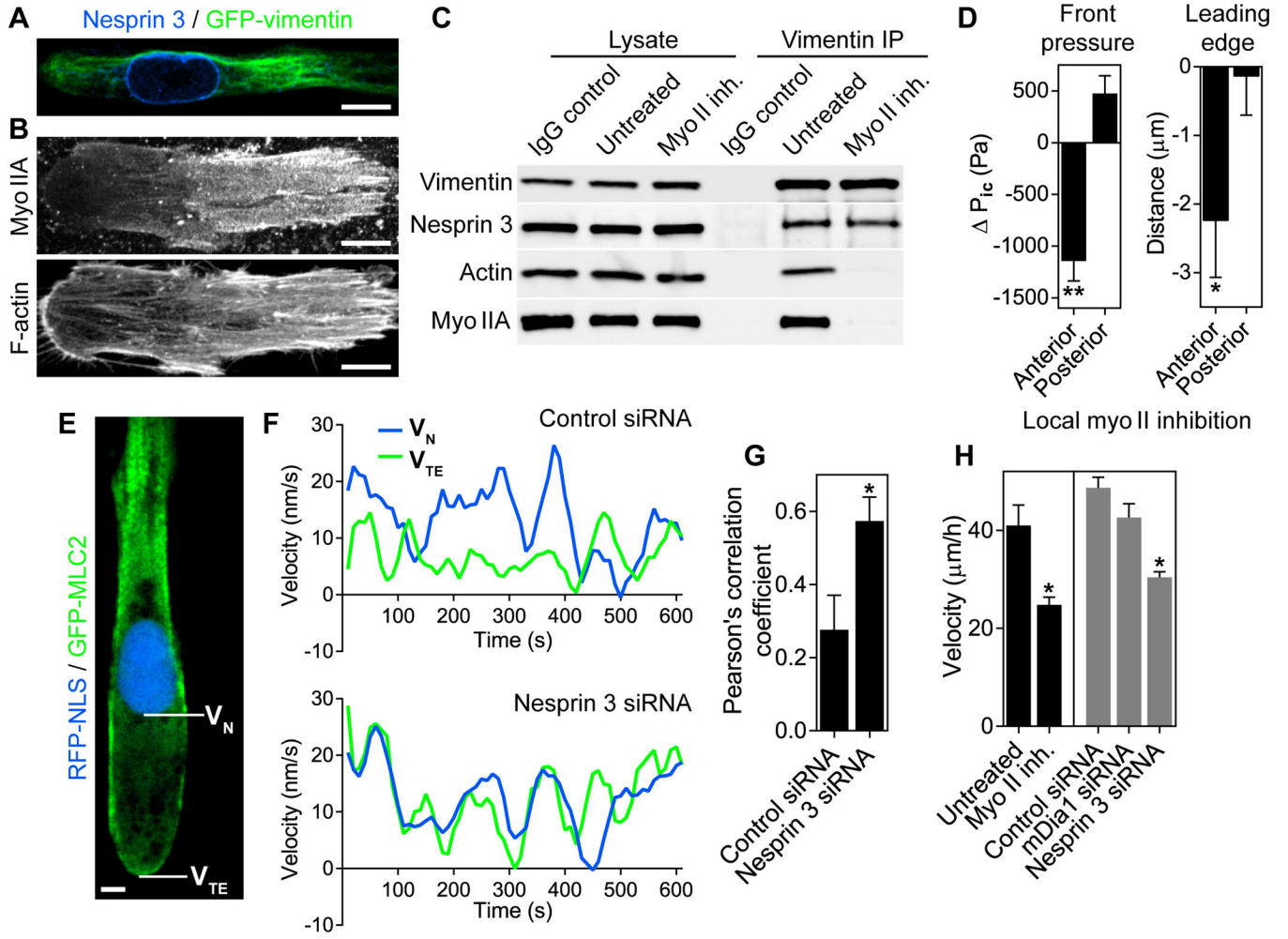


Fig. 3. Nesprin 3 associates with vimentin and actomyosin, and it mediates independent movement of the nucleus. (**A** and **B**) Filamentous vimentin (**A**) and myosin IIA (**B**) are polarized to the anterior of lobopodial fibroblasts. $n=10$. Scale bars $10\ \mu\text{m}$. (**C**) Immunoprecipitation reveals that actin and myosin IIA form a myosin II ATPase-dependent complex with vimentin and nesprin 3 in primary fibroblasts ($N=6$). (**D**) Anterior inhibition of myosin II reduces forward pressure ($n=22$, $N=3$), and the leading edge retracts ($n=27$, $N=5$). (**E–G**) Instantaneous velocities of the nucleus (V_N) and trailing edge (V_{TE}) measured in lobopodial cells ($n=14$) expressing GFP-MLC2 and RFP-NLS (**E**, scale bar $5\ \mu\text{m}$) treated with control or nesprin 3 siRNA (**F**). Nesprin 3 knockdown reduces the independent movement of the nucleus relative to the trailing edge (**G**). $N=3$. (**H**) Myosin II activity and nesprin 3 are each required for efficient 3D migration ($n=45$, $N=3$). $**P < 0.0001$, $*P < 0.05$.

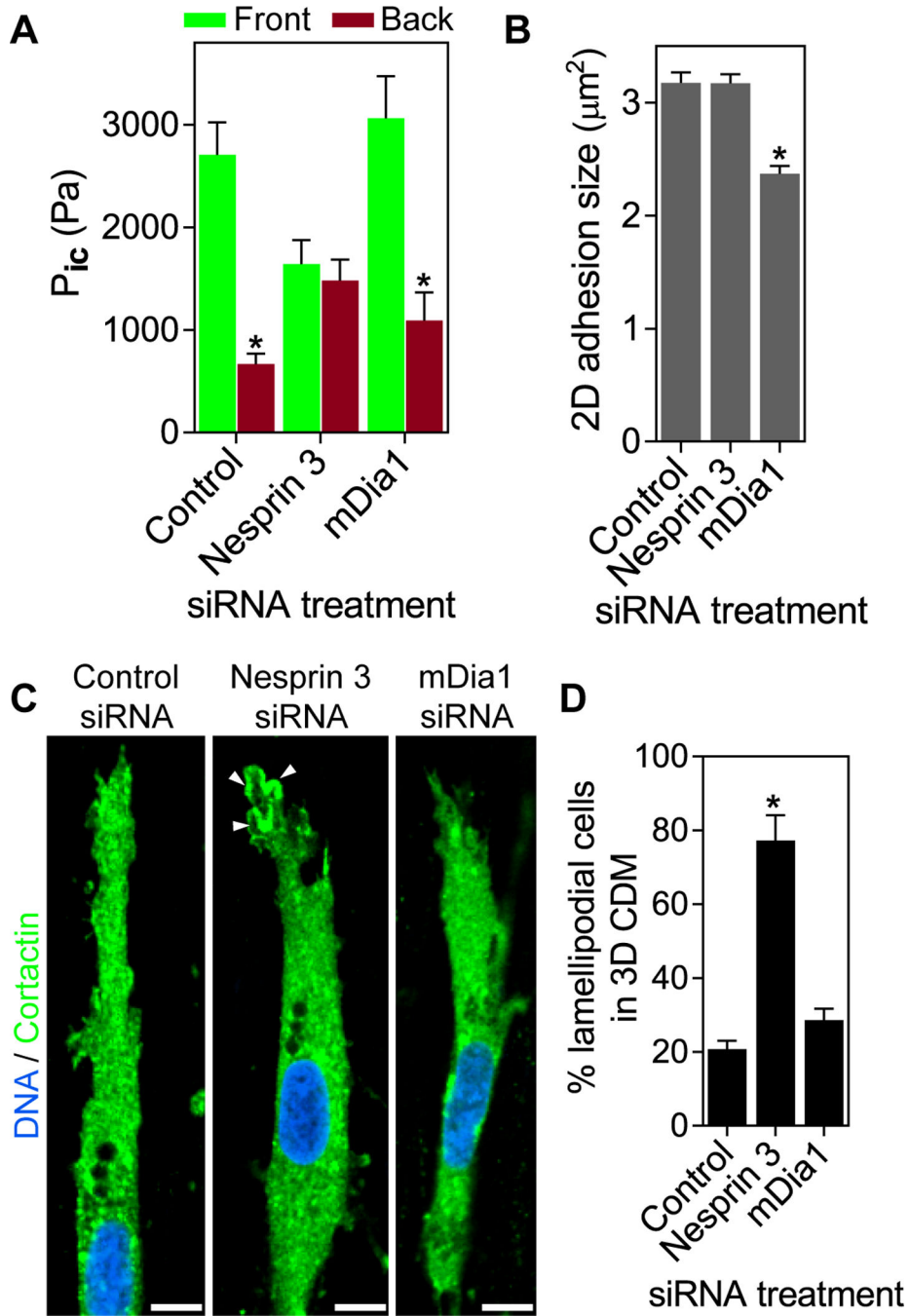


Fig. 4. Nesprin 3 compartmentalizes intracellular pressure to mediate lobopodial 3D migration. **(A)** Comparison of anterior and posterior intracellular pressure in cells treated with the indicated siRNAs (n = 23, N=3). **(B)** The average size of focal adhesions formed by cells treated with the indicated siRNAs and plated on 2D glass (n = 13, N=3). **(C)** Cortactin localization in siRNA-treated cells. n=17. Arrowheads indicate local accumulation of the lamellipodial

marker cortactin at the leading edge. **(D)** Quantification of lamellipodial cells in 3D CDM following siRNA treatments ($n = 33$, $N=3$). Scale bars 10 μm . * $P < 0.001$.

Author Manuscript

Author Manuscript

Author Manuscript

Author Manuscript